ACS APPLIED MATERIALS & INTERFACES

Research Article

www.acsami.org

Nanodrug Formed by Coassembly of Dual Anticancer Drugs to Inhibit Cancer Cell Drug Resistance

Yuanyuan Zhao,[⊥,†] Fei Chen,[⊥,†,‡] Yuanming Pan,[†] Zhipeng Li,[†] Xiangdong Xue,[†,‡] Chukwunweike Ikechukwu Okeke,[†,‡] Yifeng Wang,[†,‡] Chan Li,[†] Ling Peng,[§] Paul C. Wang,[∥] Xiaowei Ma,[*,†] and Xing-Jie Liang[*,†]

[†]Chinese Academy of Sciences (CAS), Key Laboratory for Biological Effects of Nanomaterials and Nanosafety, National Center for Nanoscience and Technology, No. 11, First North Road, Zhongguancun, Beijing 100190, China

[‡]University of Chinese Academy of Sciences, Beijing 100049, China

[§]Département de Chimie, Centre Interdisciplinaire de Nanoscience de Marseille, CNRS UMR 7325, Aix-Marseille Université, 163 Avenue de Luminy 13288, Marseille, France

[∥]Molecular Imaging Laboratory, Department of Radiology, Howard University, Washington D.C. 20060, United States

Supporting Information

ABSTRACT: Carrier-free pure nanodrugs (PNDs) that are composed entirely of pharmaceutically active molecules are regarded as promising candidates to be the next generation of drug formulations and are mainly formulated from supramolecular self-assembly of drug molecules. It benefits from the efficient use of drug compounds with poor aqueous solubility and takes advantage of nanoscale drug delivery systems. Here, a type of all-in-one nanoparticle consisting of multiple drugs with enhanced synergistic antiproliferation efficiency against drug-resistant cancer cells has been created. To nanoparticulate the anticancer drugs, 10-hydroxycamptothecin (HCPT) and doxorubicin (DOX) were chosen as a typical model. The resulting HD nanoparticles (HD NPs) were formulated by a "green" and convenient self-assembling method, and the water-solubility of 10-hydroxycamptothecin (HCPT) was improved 50-fold after nanosizing by coassembly with DOX. The formation process was studied by observing the morphological changes at various reaction times and molar ratios of DOX to HCPT. Molecular dynamics (MD) simulations showed that DOX molecules tend to assemble around HCPT molecules through intermolecular forces. With the advantage of nanosizing, HD NPs could improve the intracellular drug retention of DOX to as much as 2-fold in drug-resistant cancer cells (MCF-7R). As a dual-drug-loaded nanoformulation, HD NPs effectively enhanced drug cytotoxicity to drug-resistant cancer cells. The combination of HCPT and DOX exhibited a synergistic effect as the nanosized HD NPs improved drug retention in drug-resistant cancer cells against P-gp efflux in MCF-7R cells. Furthermore, colony forming assays were applied to evaluate long-term inhibition of cancer cell proliferation, and these assays confirmed the greatly improved cytotoxicity of HD NPs in drug-resistant cells compared to free drugs.

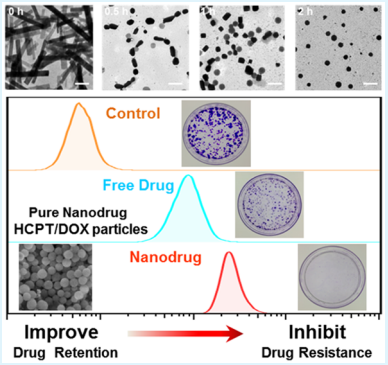

KEYWORDS: *assemble, carrier-free, pure nanodrug, drug resistance, insoluble drugs*

INTRODUCTION

Nanomedicines have attracted great interest owing to their unique properties, such as target delivery,[1−3] controllable release,[4,5] lower systematic toxicity,[6] and higher drug bioavailability.[7,8] In addition, most water insoluble drugs can be assembled into nanocarrier-based drug delivery systems to achieve much better therapeutic efficacy.[9,10] With regard to water-insoluble drug delivery, some nanocarriers have been used as described in previous reports, such as micelles and inorganic nanoparticles with the capability to solubilize drugs and deliver them to proper sites due to enhanced permeability and retention (EPR) effects.[11,12] However, concerns regarding safety problems, including potential systematic toxicity, unclear metabolism, and other uncertainties related to the use of nanocarriers, remain.[13,14] Thus, it is of great importance to develop a "green" method to create nanoformulations of drugs without the use of "toxic" solvents or nanocarriers.[15] To address these problems, we proposed carrier-free pure nanodrugs (PNDs) composed entirely of pharmaceutically active molecules as promising candidates with high expectations to deliver practicable solutions for formulation development of insoluble drugs.[16,17]

Nanoassembly technology of preparing carrier-free drug can be applied to nanoparticulate anticancer drugs and improve their therapeutic effects. 10-Hydroxycamptothecin (HCPT) and doxorubicin (DOX) are common clinical chemotherapeu-

Received: June 16, 2015
Accepted: August 13, 2015
Published: August 13, 2015

DOI: 10.1021/acsami.5b05347
ACS Appl. Mater. Interfaces 2015, 7, 19295−19305

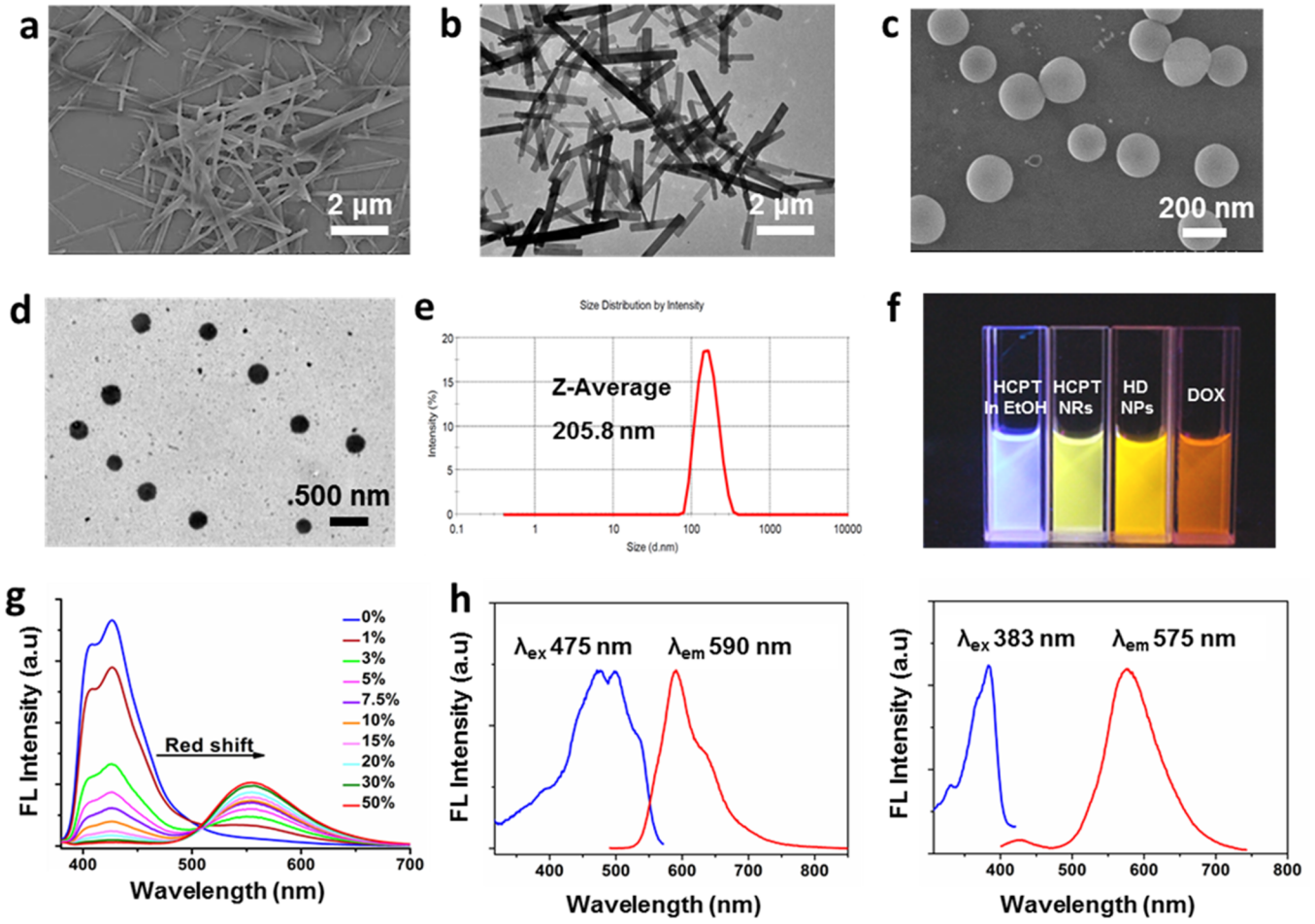

Figure 1. (a) SEM image of HCPT nanorods (NRs). (b) TEM image of HCPT NRs. (c) SEM image of HD NPs. (d) TEM image of HD NPs. (e) Size distribution of HD NPs with polydispersity index (PDI) = 0.264. (f) Fluorescence image of HCPT in ethanol, HCPT NRs in 90% water/10% ethanol, HD NPs in aqueous solution, and DOX in aqueous solution. (g) Emission spectra of HCPT in ethanol/water solution with ratios of water to ethanol from 0 to 50%. (h) Fluorescence spectra of HD NPs (20 μM DOX and 5 μM HCPT). Left: λ_{ex} (HCPT) = 383 nm. Right: λ_{ex} (DOX) = 475 nm.

tic drugs.[18,19] However, HCPT is extremely water-insoluble, and this has restricted its clinical application.[20] Traditionally, chemical modification and application of solubilizing surfactants are usually adopted to modulate the solubility.[21,22] DOX has the characteristic structure of a surfactant,[23] with the unsaturated anthracycline rings acting as the hydrophobic part and the saturated end of the ring system as a hydrophilic part, and contains abundant hydroxyl groups adjacent to the amino sugar.[24] HCPT molecules are hydrophobic;[19] therefore, we hypothesized that DOX could potentially be used for solubilizing and nanosizing HCPT. Unlike other common surfactants or non-FDA-approved nanocarriers, DOX not only acts as a cosolvent but also as a pharmaceutically active component of the final drug formulation, leading to a possible synergistic outcome of dual-drug combination therapy.[25] Conversely, by using DOX as a stabilizer in the HCPT nanosizing process, we can abandon the use of inert materials like surfactants and obtain a carrier-free dual-drug self-assembled nanostructure, namely, HCPT/DOX nanoparticles that consist exclusively of pharmaceutically active molecules. These carrier-free HCPT/DOX nanoparticles (HD NPs) are expected to help increase the amount of effective drug, reduce the dosage, and take advantage of HCPT/DOX combination therapy while avoiding biosafety uncertainties associated with conventional nanocarriers.

The synergism of supramolecular multi-interactions induces various topological structures and morphologies, which also play a vital role in carrier-free pure nanodrug formation. Usually, characteristic groups are designed for tuning the intra- and intermolecular interactions of building molecules to change and improve assembly topology. However, only a few reports describe the simple modulation of the ratio between different building molecules, especially clinically bioactive drug molecules, to construct specific nanostructures and morphologies, but it is interesting. In this work, we report a novel approach to carrier-free pure nanodrug-based combination therapy by concurrently incorporating two different types of anticancer drugs into a single drug delivery system (DDS). This dual-drug nanoparticle was formulated by tunable self-assembly, namely, exclusively from the coassembly of HCPT and DOX. The HCPT and DOX coassembled nanostructure varied from nanorods to nanospheres when the molar ratio of DOX to HCPT was changed, which also resulted in improved aqueous solubility and stability of HCPT. At a proper DOX/HCPT molar ratio, HD NPs exhibited spherical morphology and uniform sizes with excellent water dispersity and stability. The resulting pure drug nanoparticles showed much higher

DOI: 10.1021/acsami.5b05347
ACS Appl. Mater. Interfaces 2015, 7, 19295−19305

intracellular drug retention than free drugs because of their enhanced internalization rates and inhibition to P-gp mediated drug efflux. Moreover, codelivery of HCPT and DOX via a single nanoparticle showed significant synergy in the efficacy of these agents. Cellular cytotoxicity and colony forming assays indicated that HD NPs can effectively improve anticancer drug efficacy and enhance inhibition to drug-resistant cancer cells. These results indicated that a carrier-free pure nanodrug platform obtained from self-assembly can offer new means for combating cancer cell drug resistance by building synergy through combination chemotherapy and inhibiting P-gp drug efflux.[20]

RESULTS AND DISCUSSION

Morphology Regulation of HD Particles from Nanorods to Nanospheres. HCPT is known to have poor solubility in water; thus, its ethanol solution was prepared. When diluted into Milli-Q water, HCPT solution shows a clear Tyndall light-scattering effect (Figure S1),[26] which is induced by self-assembly of planar HCPT molecules.[16,27] The assembled HCPT particles exhibited a stable rodlike morphology, which is characterized by a transmission electron microscope (TEM) and scanning emission microscope (SEM) (Figure 1a and 1b). When DOX·HCl aqueous solution was added to an HCPT suspension (DOX/HCPT molar ratio = 4:1), DOX·HCl molecules coassembled with the present nanorods and formed spherelike HD nanoparticles composed of HCPT and DOX·HCl molecules with sizes around 200 nm (Figure 1c–e). The fluorescence of HCPT changed from blue in ethanol solution to green in ethanol/water solution (Figure 1f), which may be explained by efficient excited-state proton transfer (ESPT).[27] When we examined the fluorescence spectrum of HCPT in a water/ethanol mixture, an obvious red-shift of the emission maximum was observed as the water fraction increased, and the emission maximum was shifted from blue (λ_{ex}= 382 nm, λ_{em}= 427 nm) to green (λ_{ex}= 382 nm, λ_{em}= 550 nm) (Figure 1g). HD NP solution showed orange colored fluorescence as a result of the merge of HCPT and DOX fluorescence (Figure 1f). The coassembled particles showed both red light emission (DOX) and green light emission (HCPT) (Figure 1h), which implied that the particles were composed of both HCPT and DOX. Moreover, confocal laser scanning fluorescent microscopy (CLSM) images (Figure S2) showed colocalization of the green and red fluorescence, which confirmed that HCPT and DOX were doped with each other in one single particle. In addition, the surface charge of the resulting HD NPs was +29.1 mV, whereas that of HCPT nanorods was −12.1 mV (Figure S3), which also indicated the coassembly of DOX and HCPT. The dramatic shift of surface charge was probably because the NH^{3+} groups of the DOX molecules were located on the surface of the HD NPs, which would be helpful for stabilizing the particles.

Molecular dynamics (MD) simulations were performed on HCPT and DOX to help understand how the molecules would interact with each other in aqueous solution. MD simulation predicted that HCPT molecules, when initially arranged apart, rapidly self-assembled into a stacklike structure in water, as shown in Figure 2a. This configuration formed within 10 ns and was then stably maintained.[16] Next, DOX molecules were added to the simulation and arranged apart from the HCPT stack. After 50 ns, the DOX molecules were predicted to coassemble with the HCPT molecules, as shown in Figure 2b. The final structure is likely to be held together by a synergetic

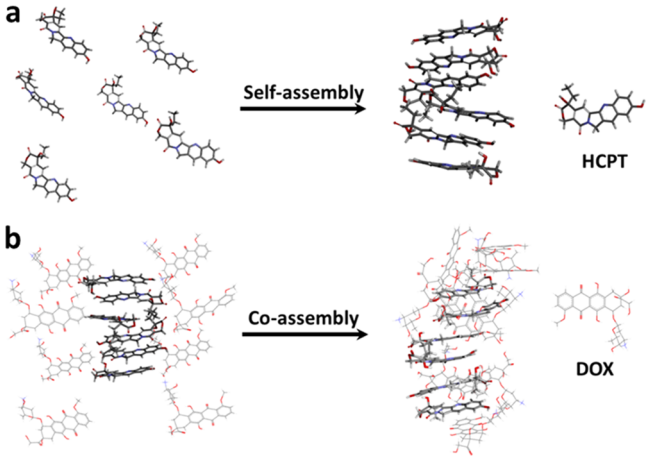

Figure 2. (a) MD simulations of the self-assembly of HCPT molecules in water after 10 ns. (b) MD simulations of the coassembly of HCPT and DOX molecules in water after 50 ns. The software is VMD.

supramolecular interaction, including $\pi-\pi$ stacking and hydrophobic interactions, supported by the analysis of DS 4.0 (Figure S4).[23] The predictions from these MD simulations are consistent with our experimental data and strongly support the hypothesis that HCPT and DOX molecules coassembled into HD NPs.

The size and morphology of the coassembled particles were influenced by reaction time and the molar ratio of DOX to HCPT. The formation processes of HD nanoparticles and reassembly were monitored in detail by TEM at different time points (0, 0.5, 1, and 2 h). As shown in Figure 3a, HCPT nanorods became smaller in size after the addition of DOX and passed through the morphology transitions from rodlike and squarelike to spherelike particles. It could be explained that DOX molecules interacted with HCPT nanorods and caused the disassembly of HCPT nanorods and then led to the coassembly of added DOX and original HCPT nanorods to a kind of spherical HCPT/DOX particle gradually. Moreover, the molar ratio of DOX to HCPT also affected the polydispersity index (PDI) and morphology of the obtained HD NPs. As the molar ratio of DOX to HCPT increased from 0 to 4:1, the average hydrodynamic diameter of the composite HD particles decreased from 2.5 μm to 205.8 nm, and the PDI decreased from 1 to 0.219 (Figure 3b), which implied changes in the assembly morphology. When the DOX/HCPT ratio was 8:1, HD particles with a hydrodynamic diameter of 163.3 nm were obtained, but the PDI was as high as 0.545, implying that the particle size distribution was too broad to be suitable for further experiments. SEM images demonstrated the gradual transition of morphology with the molar ratio (0.5:1, 2:1, and 4:1) (Figure 3c). When the molar ratio was 0.5:1, HCPT and DOX assembled to rodlike HD particles. As the molar ratio increased to 2:1, more obvious changes in morphology were observed, and most of the HCPT/DOX assemblies exhibited rectangular- or squarelike morphologies. Finally, at the optimized molar ratio (4:1), spherically assembled particles (HD NPs) with uniform size and suitable polydispersity were obtained (Figures 1c–e and 3b), and we chose this ratio for further investigation. In summary, by rapidly injecting an aqueous solution of DOX into a suspension of HCPT nanorods at a molar ratio of 4:1 (DOX to HCPT), HD particles with suitable size and shape could be prepared. All of the solvents and materials used in the preparation are approved by the Food and Drug Administration

DOI: 10.1021/acsami.5b05347
ACS Appl. Mater. Interfaces 2015, 7, 19295–19305

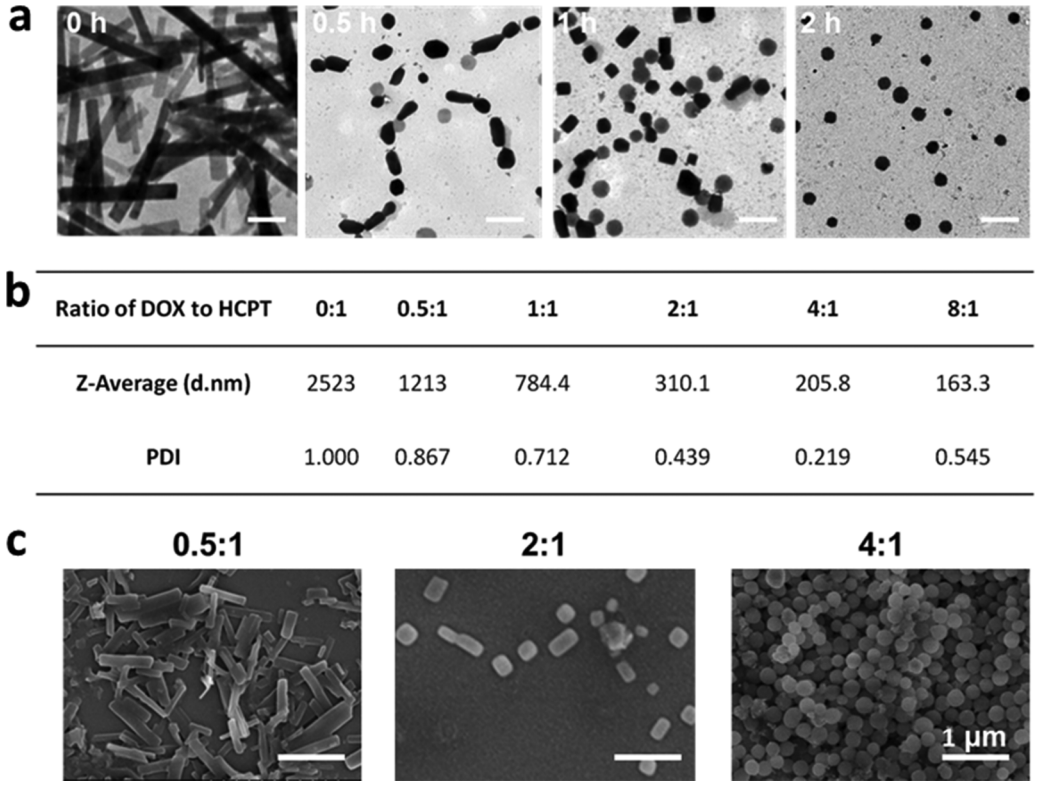

Figure 3. (a) HD NP formation process from nanorods to nanospheres characterized by TEM at different time points (0, 0.5, 1, and 2 h). The scale bar is 500 nm. (b) Particle size distribution and polydispersity index (PDI) of particles generated from different molar ratios of DOX to HCPT (0:1, 0.5:1, 1:1, 2:1, 4:1, and 8:1). (c) SEM images of HCPT/DOX particles assembled from different molar ratios of DOX to HCPT (0.5:1, 2:1, and 4:1). The scale bar is 1 μm. When the ratio of DOX to HCPT is low, HCPT nanorods tend to form, but when the ratio of DOX to HCPT is high, spherical HD NPs are formed.

(FDA). The obtained HD NPs consisting of two anticancer drugs were suitable for both HCPT and DOX delivery.

It is worth noting that the DOX molecules acted as a special surfactant-like cosolvent and improved the water dispersity and stability of HCPT assembled particles in solution during the coassembly process. The stability of HD NPs was not affected by being lyophilized and redissolved in water (Figure S5), and the concentration of HCPT in the dispersed solution of HD NPs can be as high as 325.3 μg/mL, nearly 50-fold higher than the solubility of free drug in water (HCPT = 7.28 μg/mL).[28,29] For further pharmaceutical studies, the stability and drug release of HD NPs was first investigated. It was already known that HD NPs had both the fluorescence of HCPT (green) and DOX (red), as shown in Figure S2. Therefore, to test the stability of HD NPs, 10% fetal bovine serum (FBS) was used to incubate HD NPs at 37 °C for 2 h, and then their fluorescence was observed by confocal microscopy. The results showed that HD NPs exhibited both the fluorescence of HCPT and DOX and kept their integrity, indicating that HD NPs remained stable in 10% FBS (Figure S2). Moreover, HCPT and DOX could be released from HD particles in a lysosomal environment (pH 5.0). As shown in Figure 4a, compared with free drug, both the fluorescence of HCPT and DOX in HD NPs was significantly reduced. At pH 7.4, HCPT NRs and DOX coassembled to nanospheres and kept balance between the orignal negative HCPT NRs and positive DOX·HCl molecules (Figure 4b); at pH 5.0, the fluorescence intensity of both HCPT and DOX increased, implying the balance was broken, and drugs were released from HD NPs (Figure 4b). As shown in Figure 4c, HD NPs showed different fluorescence in physiological pH (PBS buffer, pH 7.4) and acidic pH circumstances (PBS buffer, pH 5.0). When HD NPs were dispersed in acidic pH circumstances, the fluorescence of DOX ("red" color) was restored, which means some of the DOX was detached from HD NPs. Moreover, when the pH of the HD NP solution was changed to 5.0 from 7.4, the Tyndall effect became significantly weakened, which confirmed that the HD NPs decomposed and some drug molecules had detached from the HD NPs, dispersing throughout the solution. On the basis of these in vitro experiments, we hypothesized that after HD NPs were taken up by cells, DOX and HCPT molecules would be released due to the low internal pH of lysosomes. The stability and drug release properties of the obtained HD spheres would benefit subsequent studies based on their pharmacological function.

HD NPs Show Improved Cellular Drug Accumulation by Drug-Resistant Cancer Cells. Breast cancer is the most common cancer and the leading cause of cancer death in women worldwide,[30,31] and overcoming the multidrug resistance of breast cancer developed during chemotherapy, especially in metastatic and advanced forms, is vital for effective therapy.[32,33] High cellular expression of P-gp results in multidrug resistance (MDR) in vitro and is believed to be a clinically relevant mechanism for tumor resistance to chemotherapy.[34,35] The MCF-7R cell line is drug resistant partly due to the overexpression of P-gp protein,[36] which functions as an active efflux pump for many structurally diverse lipophilic compounds, such as DOX and HCPT. The level of P-gp in breast cancer cells was confirmed by both confocal immunofluorescent analysis and Western blot experiments. Rhodamine-

DOI: 10.1021/acsami.5b05347
ACS Appl. Mater. Interfaces 2015, 7, 19295−19305

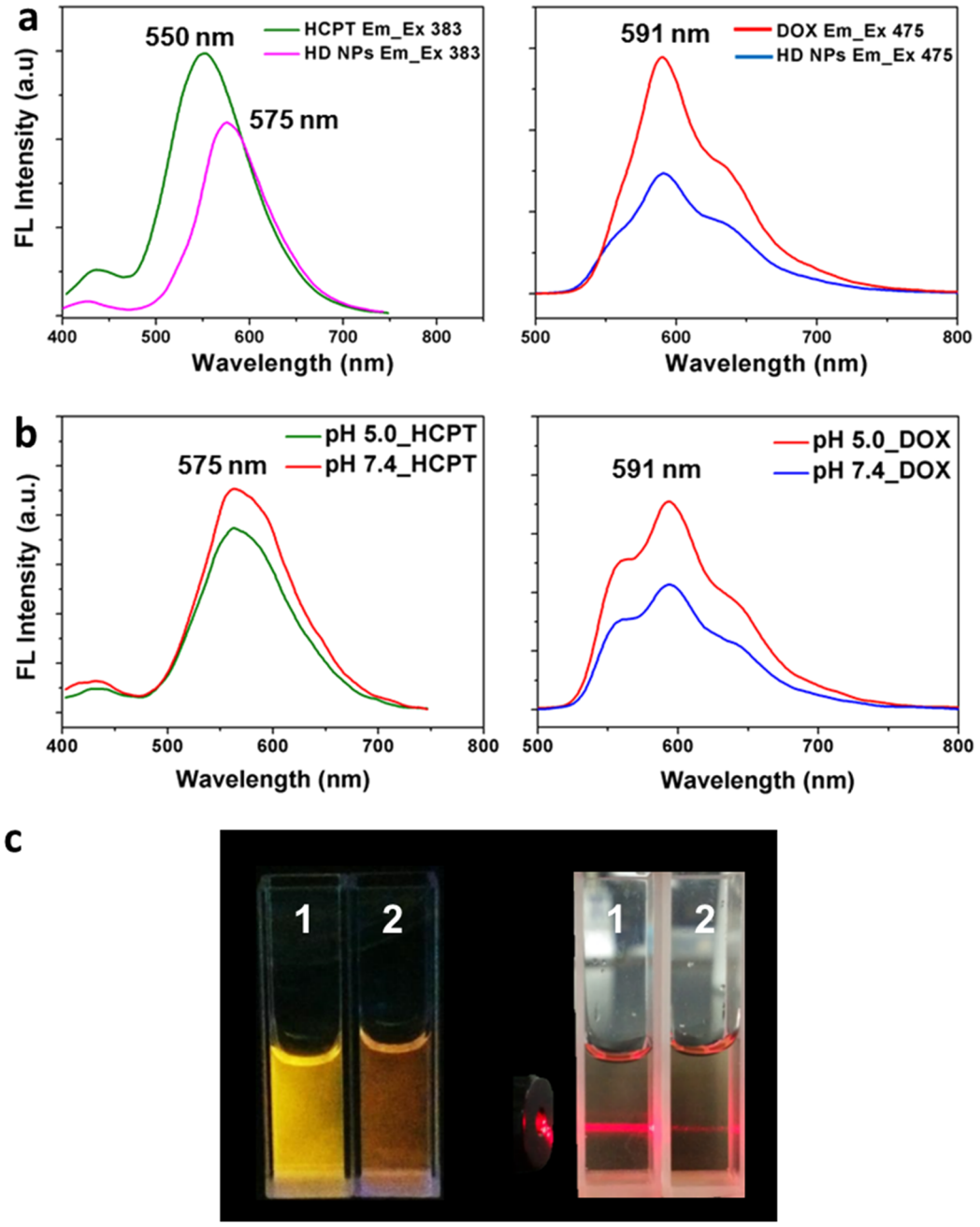

Figure 4. (a) Fluorescence spectra of DOX, HCPT, and HD NPs (20 μM DOX and 5 μM HCPT). λex (HCPT) = 383 nm. λex (DOX) = 475 nm. (b) Changes in the fluorescence spectra of 20 μM HD NPs (20 μM DOX and 5 μM HCPT) when dispersed in pH 7.4 and pH 5.0 PBS buffer. λex (HCPT) = 383 nm. λex (DOX) = 475 nm. (c) Fluorescence pictures and Tyndall effect of 1 (20 μM HD NPs in PBS buffer, pH 7.4) and 2 (20 μM HD NPs in PBS buffer, pH 5.0).

labeled antibody was used to detect the distribution of P-gp expression by confocal microscopy (Figure S6a). The fluorescence intensity of rhodamine is positively related to the amount of P-gp. The cross-linked filaments that are uniformly distributed in the cytoplasm of MCF-7R cells correspond to stained P-gp protein. The confocal images showed that the level of P-gp was much higher in drug-resistant MCF-7R cells compared to sensitive MCF-7S cells (Figure S6a). This is consistent with the results of a Western blot experiment (Figure S6b), which showed that there was a high level of P-gp expression in drug-resistant MCF-7R cancer cells.

Overexpression of P-gp protein is one of the main reasons for cancer cell drug resistance, because P-gp-mediated drug efflux can strongly decrease the effective drug concentration in cancer cells. However, in our work, the HD NPs could effectively enhance internalization rates and improve intracellular drug accumulation, which was demonstrated by the results of confocal microscopy and flow cytometry quantification. DOX and HCPT are self-luminescent molecules; thus, the HD NPs can be conveniently tracked in cells as a self-indicating drug delivery system by fluorescence microscopy. Emission at 500−550 nm (green color) with excitation at 405 nm was chosen for fluorescence detection of HCPT, and 590−650 nm emission (red color) with 488 nm excitation was chosen for detection of DOX. Because of the P-gp-mediated drug efflux, HCPT and DOX could barely stay inside the drug-resistant

DOI: 10.1021/acsami.5b05347
ACS Appl. Mater. Interfaces 2015, 7, 19295−19305

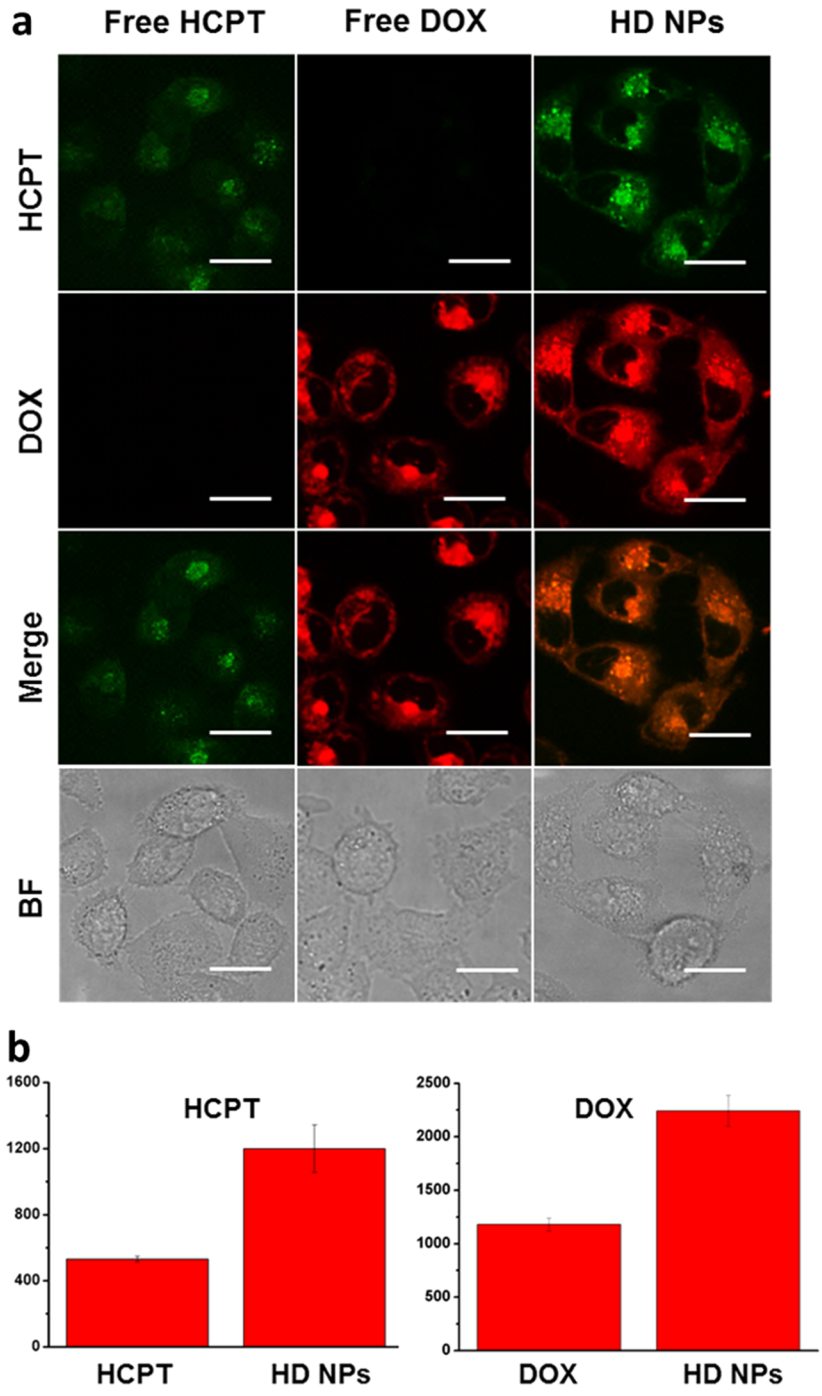

Figure 5. (a) Confocal images of MCF-7R breast cancer cells after incubation with free HCPT (10 μM), free DOX (40 μM), and HD NPs (40 μM DOX and 10 μM HCPT) for 4 h. Scale bars are 30 μm. BF, bright field images. (b) Mean fluorescence intensity of MCF-7R cells incubated with free DOX, free HCPT, and HD NPs. Cells treated with HD NPs take up more HCPT than cells treated with free HCPT; $p < 0.05$.

cells, and cells treated with HCPT or DOX showed weak fluorescence (Figure 5a). However, cells treated with HD nanoparticles showed strong colocalized HCPT and DOX fluorescence, which was much stronger than free-drug treated cells. By analyzing the fluorescence intensity, it was indicated that HD NPs improved the intracellular drug concentration of both HCPT and DOX (Figure 5b). These results indicated that the dual-drug-loaded HD NPs were more efficient at delivering drug molecules into drug-resistant cells and may therefore lead to a better therapeutic outcome. Flow cytometry measurements were also taken to confirm the higher accumulation of HD NPs in drug-resistant cells. As shown in Figure 6a, HD NPs promoted the accumulation of both HCPT and DOX in drug-resistant MCF-7R cells compared to free HCPT and DOX. To test the property of HD NPs in promoting cellular uptake and inhibiting P-gp-mediated drug efflux, we further detected the difference in the intracellular drug concentration between the HD NPs (drug nanoparticle) and DOX (free drug). Cells were preincubated with free DOX or HD NPs for 1 h, and then each sample was divided into two aliquots. One aliquot was used to quantify the amount of DOX inside cells after 1 h of preincubation (A, DOX; C, HD NPs). For the other aliquot,

DOI: 10.1021/acsami.5b05347
ACS Appl. Mater. Interfaces 2015, 7, 19295−19305

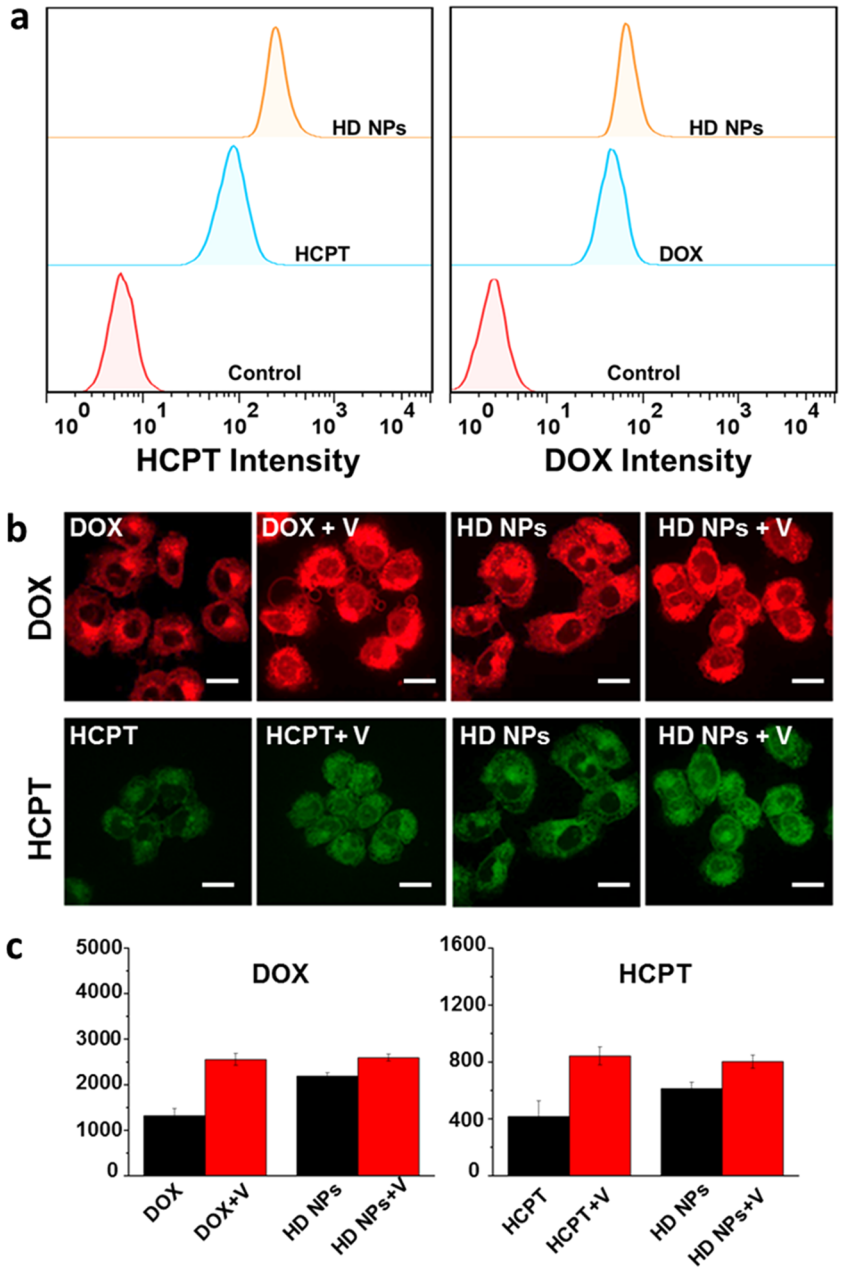

Figure 6. (a) Flow cytometry measurements of the uptake of DOX and HCPT by MCF-7R cells after incubation with free DOX, free HCPT, and HD NPs (40 μM DOX and 10 μM HCPT) for 4 h. (b) Confocal images of MCF-7R cells incubated with DOX, DOX + verapamil, HCPT, HCPT + verapamil, HD NPs, HD NPs + verapamil (DOX 40 μM, HCPT 10 μM, and verapamil 100 μM) for 4 h. V means verapamil. Scale bars are 30 μm. (c) Fluorescence intensity determined from the confocal results in (b).

incubation was continued in drug-free medium for another 4 h before the amount of DOX was measured (B, DOX; D, HD NPs). Flow cytometry analysis was conducted to quantify the intracullur drug level, and the efflux amount of DOX was shown by comparing the intracellular drug intensity of cells before and after the 4 h incubation period. As shown in Figure S7a, the amount of DOX pumped out by P-gp during the 4 h was determined by the decrease in DOX intensity from A to B (Efflux 1, cells treated with free DOX) or C to D (Efflux 2, cells treated with HD NPs). Obviously, Efflux 2 was lower than Efflux 1, indicating that HD NPs inhibited the efflux of DOX and therefore led to higher drug retention. The quantification data derived from the flow cytometry analysis (Figure S7b) indicated that the effective drug retention in MCF-7R cells almost doubled from 10.40% (free drug) to 19.82% (HD NPs), which was consistent with the confocal results. We inferred that nanoscale delivery system-based HD NPs had the property of higher cellular uptake. In addition, HD NPs effectively improved the solubility of HCPT and resulted in increased cellular uptake, whereas free HCPT was insoluble in water. Moreover, nanoparticles were regarded to be effective in inhibiting drug efflux because P-gp could not pump out nanoscale-sized particles.

Promoted Uptake and Reduced Efflux Contribute to the Higher Drug Retention of HD NPs in MCF-7R Cells. As we know, nanoparticles are not a substrate of P-gp protein and cannot be pumped out by P-gp;[36] therefore, no efflux of intact HD NPs from MCF-7R cells is expected. However,

DOI: 10.1021/acsami.5b05347
ACS Appl. Mater. Interfaces 2015, 7, 19295−19305

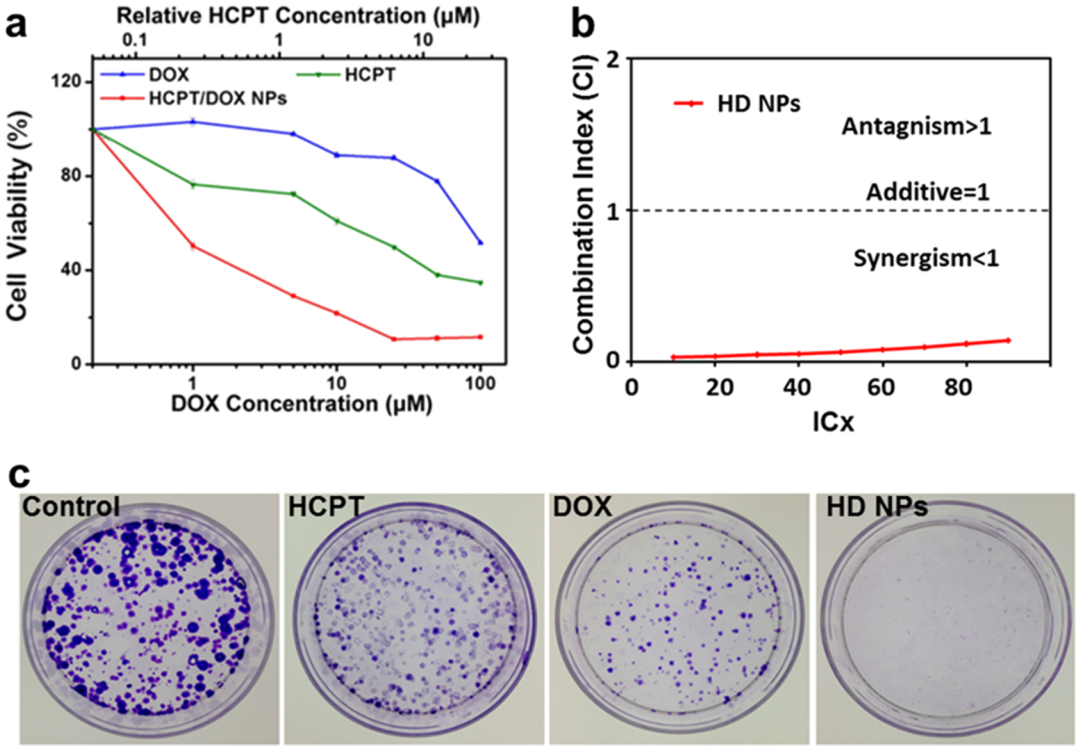

Figure 7. a) Cytotoxicity of HD NPs, free DOX, and free HCPT toward MCF-7R cells evaluated by CCK-8 assays after 48 h of treatment. (b) Combination index (CI) of HD NPs against MCF-7R cells. CI values <1 indicate synergism, CI values equal to 1 indicate an additive effect, and CI values >1 indicate antagonism. (c) Long-term colony formation assays of MCF-7R cells. Cells were grown in the presence of drugs (4 μM DOX and 1 μM HCPT) for 7 days. For each cell line, all dishes were fixed at the same time, stained, and photographed.

within the complex intracellular environment, some of HD NPs may readily break apart to release free drug molecules, which could then be easily pumped out by P-gp. Thus, HD NPs could only partially inhibit drug efflux. However, it was still significant in combating cancer cell drug resistance because higher therapeutic efficacy could be achieved by the doubled intracellular drug retention of HD NPs.

To further study the influence of cellular uptake and drug efflux of HD NPs by P-pg in drug-resistant cancer cells, we adopted verapamil as a P-gp inhibitor. Verapamil is a calcium channel blocker[37,38] that has been shown to enhance retention of antitumor agents through competition for closely related binding sites on P-pg.[37] In this way, it reverses drug resistance and restores the sensitivity of cancer cells to anticancer drugs. Verapamil was used to inhibit the activity of P-gp in MCF-7R cells; then, the intracellular drug retention of NPs was studied by confocal and flow cytometry analysis. Cells were preincubated with verapamil for 4 h, and then free HCPT, free DOX, and HD NPs were added for another 4 h incubation. Cells were then collected for confocal observation (Figure 6b). As shown in Figure 6b, verapamil inhibited the function of P-gp and thus improved the intracellular accumulation of free DOX and free HCPT. After inhibition of the P-gp function, there was an increase in drug accumulation in MCF-7R cells, which should be negatively related to drug efflux by P-gp. The results in Figure 6c show that HD NPs could decrease drug efflux and promote cellular uptake, which led to higher drug retention of HD NPs in drug-resistant cells compared to free drugs. These results indicated that nanosized drugs with nanostructure could effectively decrease the drug efflux action of the P-gp. Together, these results suggest that both the higher uptake and decreased efflux of the nanostructured drug contribute to the final higher retention of drugs by cells treated with nanosized HD NPs.

Synergistic Inhibition of HD NPs to Drug-Resistant Cancer Cells in Cell Counting Kit-8 (CCK-8) and Colony Forming Assay (CFA). To further explore the anticancer effect of HD NPs, we went on to evaluate their inhibition efficiency to MCF-7R cells by CCK-8 assays and colony forming assays (Figure 7). Here, the in vitro cytotoxicity of HD NPs, free HCPT, and free DOX to MCF-7R cells was evaluated by CCK-8 assays. Cells were incubated with various concentrations of HCPT, DOX, and HD NPs in culture medium. Compared to free DOX and free HCPT, HD NPs showed much higher toxicity to MCF-7R cells at the same concentration (Figure 7a). Significantly, the combination index of HD NPs was 0.142 (Figure 7b). A combination index of <1 indicates that drugs are acting synergistically; thus, the observed value of 0.142 provides evidence that HCPT and DOX, when combined in HD NPs, synergize strongly to reduce the viability of MCF-7R cells. This is in contrast to the reported antagonism or additive effect between free HCPT and free DOX when they are administered simultaneously.[39]

Next, we used the colony forming assay (CFA) to compare the ability of HD NPs and free drugs to prevent the proliferation of MCF-7R cells. The CFA is an extensively used and well-established method for testing chemotherapeutic agents in vitro.[40] MCF-7R cells were treated with HD NPs, free DOX, or free HCPT for 7 days. Each colony is derived from a single cell, and therefore, the CFA reflects the ability of chemotherapeutic agents to prevent the cells from dividing. Significantly fewer colonies survived on the plates exposed to HD NPs than on the plates treated with free DOX or free HCPT (Figure 7c). Thus, the nanostructured HD NPs were

DOI: 10.1021/acsami.5b05347
ACS Appl. Mater. Interfaces 2015, 7, 19295−19305

more effective than the free drugs in overcoming the drug resistance of MCF-7R cells.

As reported, a TOP 1 inhibitor will increase the sensitivity of cancer cells if they are TOP 2 resistant and vice versa.[41,42] Therefore, we hypothesized that a combination of HCPT (TOP 2 inhibitor) and DOX (TOP 1 inhibitor) could restore the sensitivity of MCF-7R to anticancer drugs and enhance the therapeutic efficacy. HD NPs showed the most potent inhibition of proliferation of drug-resistant MCF-7R cancer cells, implying that dual-drug nanoparticles have potential not only in efficient drug delivery but also in combination therapy with synergistic effects to combat the drug resistance of cancer cells. This study emphasizes that the key points of designing nanosized carrier-free drugs to overcome drug resistance are to improve cellular uptake and lower the efflux of drugs from the cytoplasm of drug-resistant cancer cells through tuning parameters such as size, surface charge, and so forth.

CONCLUSIONS

In summary, HCPT was nanosized with the assistance of DOX to fabricate carrier-free HCPT/DOX nanoparticles using a simple "green" preparation procedure. DOX and HCPT molecules tend to coassemble through $\pi-\pi$ stacking interactions and form nanostructures, which are affected by reaction time and their molar ratio. At a proper molar ratio and reaction time, HD NPs exhibit uniform sizes and spherelike morphology with good stability. In addition, this nanosizing method successfully improves the water-solubility of HCPT. The obtained HD NPs, which contain two drugs assembled into one single particle, show a synergistic therapeutic effect due to higher chemosensitization induced by the HCPT/DOX combination and improved intracellular drug accumulation, which also showed significant clinic guidance and enlightenment. Furthermore, the HD NPs showed enhanced inhibition to drug-resistant cancer cells due to the obvious increase in drug retention. Our work reveals that when chemotherapeutic drugs are combined appropriately according to their properties, they can form nanoparticles through intermolecular forces. We have proposed a pure drug nanosizing technology that has potential promise in future clinical practice, especially in solubilizing water-insoluble drugs and overcoming chemotherapeutic resistance.

MATERIALS AND METHODS

Materials. Doxorubicin hydrochloride was purchased from Hisun Pharmaceutical Corp (Taizhou, Zhejiang, China) and 10-hydroxycamptothecin was purchased from Knowshine (Shanghai, China). Ethanol was bought from AMRESCO (Solon, OH, USA). Water was purified using a Milli-Q system (Millipore, Milford, MA, USA). Unless otherwise noted, all chemicals were used as received without further purification, and Milli-Q water (18.2 MΩ·cm, Millipore System Inc.) was used throughout this study.

Preparation of HCPT/DOX Nanoparticles (HD NPs). HD NPs were prepared by the reprecipitation method. First, 2 mL of water was heated to 50 °C, and 200 μL of HCPT (1 mM) in ethanol was dropped into it under continuous stirring. Forty microliters of an aqueous solution of DOX (10 mM) was then added, and the obtained mixture was stirred for another 2 h.

Evaluation of Cell Viability by CCK-8 Assays. CCK-8 assays were used to assess the viability of MCF-7R cells after exposure to HD NPs, DOX, and HCPT. MCF-7R cells were seeded onto 96-well plates at a density of 4,000 cells per well and cultured overnight until the cells were fully attached. Increasing concentrations of HCPT, DOX, and HD NPs in medium (HCPT: 0.25, 1.25, 2.5, 6.25, 12.5, and 25 μM; DOX: 1, 5, 10, 25, 50, and 100 μM) were added to each well. Control cells were grown in medium without further treatment. After 48 h, 10 μL of CCK-8 solution was added to each well, and the cells were further incubated for 2 h at 37 °C. The plates were then analyzed with a microplate reader (Tecan Infinite M200, USA) with the absorbance set at 450 nm. As a reference, the absorbance at 630 nm was also measured. The experiments were performed at least 3 times.

Synergistic Effect Evaluated by Combination Index. The degree of synergy between two drugs can be quantified by calculating the combination index (CI). The CI of HCPT and DOX when combined in HD NPs was calculated from the dose−effect profiles according to the equation: CI = D1/Dm1 + D2/Dm2, where D1 and D2 are the concentrations of drug 1 and drug 2, respectively, that in combination produce a certain level of cytotoxicity, and Dm1 and Dm2 are the concentrations of the single drugs, administered separately, that produce the same effect. CI values <1 indicate synergism, CI values equal to 1 indicate an additive effect, and CI values >1 indicate antagonism.

Uptake of DOX and HCPT Measured by Flow Cytometry. HCPT (10 μM) and HD NPs (40 μM DOX and 10 μM HCPT) for 2 h, and 10,000 cells were seeded into 6-well culture plates and incubated for 12 h, and then incubated with free DOX (40 μM), free HCPT (10 μM), and HD NPs (40 μM DOX for another 4 h). After harvesting, cells were washed with PBS, and the fluorescence was measured using a Beckman Coulter Cell Lab Quanta SC with excitation wavelengths of 405 and 488 nm. Fifteen thousand cells were counted.

Uptake of DOX- and HCPT-Measured Confocal Microscopy Imaging. Ten thousand MCF-7R cells were seeded into 35 mm glass-bottom dishes. After 24 h, the cells were treated with DOX, HCPT, and HD NPs (40 μM DOX and 10 μM HCPT) for 4 h. The cells were examined by confocal microscopy (Zeiss LSM 760 fluorescence spectrophotometer, Germany). DOX was excited by a 488 nm laser, and HCPT was excited by a 405 nm laser.

ASSOCIATED CONTENT

Supporting Information

The Supporting Information is available free of charge on the ACS Publications website at DOI: 10.1021/acsami.5b05347.

Methods, including characterization of HD NPs, cell culture, and colony forming assay, additional figures, including zeta potential, confocal images, molecular interaction analysis data, and so forth (PDF)

AUTHOR INFORMATION

Corresponding Authors

*E-mail: maxw@nanoctr.cn (X.M.).

*E-mail: liangxj@nanoctr.cn. Tel.: +86-10-82545569. Fax: +86-10-62656765 (X.-J.L.).

Author Contributions

⊥These authors contributed equally to this work.

Notes

The authors declare no competing financial interest.

ACKNOWLEDGMENTS

This work was supported by the National Natural Science Foundation of China (Projects 81201194, 31570968, and 31430031), Beijing Natural Science Foundation (7152157), National Distinguished Young Scholars grant (31225009), State High-Tech Development Plan (2012AA020804 and 2014AA020708), and Special Financial Grant from the China Postdoctoral Science Foundation (2013T60089). The authors also appreciate support by the "Strategic Priority Research Program" of the Chinese Academy of Sciences, Grant No. XDA09030301, and support by the external cooperation

DOI: 10.1021/acsami.5b05347
ACS Appl. Mater. Interfaces 2015, 7, 19295−19305

program of BIC, Chinese Academy of Science, Grant No. 121D11KYSB20130006.

REFERENCES

(1) Montenegro, J. M.; Grazu, V.; Sukhanova, A.; Agarwal, S.; de la Fuente, J. M.; Nabiev, I.; Greiner, A.; Parak, W. J. Controlled antibody/(bio-) Conjugation of Inorganic Nanoparticles for Targeted Delivery. *Adv. Drug Delivery Rev.* **2013**, *65*, 677−688.
(2) Bhirde, A. A.; Chikkaveeraiah, B. V.; Srivatsan, A.; Niu, G.; Jin, A. J.; Kapoor, A.; Wang, Z.; Patel, S.; Patel, V.; Gorbach, A. M.; Leapman, R. D.; Gutkind, J. S.; Hight Walker, A. R.; Chen, X. Targeted Therapeutic Nanotubes Influence the Viscoelasticity of Cancer Cells to Overcome Drug Resistance. *ACS Nano* **2014**, *8*, 4177−4189.
(3) Zhen, Z.; Tang, W.; Chen, H.; Lin, X.; Todd, T.; Wang, G.; Cowger, T.; Chen, X.; Xie, J. RGD-modified Apoferritin Nanoparticles for Efficient Drug Delivery to Tumors. *ACS Nano* **2013**, *7*, 4830−4837.
(4) Ganta, S.; Devalapally, H.; Shahiwala, A.; Amiji, M. A Review of Stimuli-responsive Nanocarriers for Drug and Gene Delivery. *J. Controlled Release* **2008**, *126*, 187−204.
(5) Junghanns, J. U.; Muller, R. H. Nanocrystal Technology, Drug Delivery and Clinical Applications. *Int. J. Nanomed.* **2008**, *3*, 295−309.
(6) Fang, R. H.; Hu, C. M.; Luk, B. T.; Gao, W.; Copp, J. A.; Tai, Y.; O'Connor, D. E.; Zhang, L. Cancer Cell Membrane-coated Nanoparticles for Anticancer Vaccination and Drug Delivery. *Nano Lett.* **2014**, *14*, 2181−2188.
(7) Xu, X. Y.; Xie, K.; Zhang, X. Q.; Pridgen, E. M.; Park, G. Y.; Cui, D. S.; Shi, J. J.; Wu, J.; Kantoff, P. W.; Lippard, S. J.; Langer, R.; Walker, G. C.; Farokhzad, O. C. Enhancing Tumor Cell Response to Chemotherapy through Nanoparticle-mediated Codelivery of siRNA and Cisplatin Prodrug. *Proc. Natl. Acad. Sci. U. S. A.* **2013**, *110*, 18638−18643.
(8) Wei, T.; Liu, J.; Ma, H.; Cheng, Q.; Huang, Y.; Zhao, J.; Huo, S.; Xue, X.; Liang, Z.; Liang, X. J. Functionalized Nanoscale Micelles Improve Drug Delivery for Cancer Therapy in vitro and in vivo. *Nano Lett.* **2013**, *13*, 2528−2534.
(9) Pelaz, B.; Jaber, S.; de Aberasturi, D. J.; Wulf, V.; Aida, T.; de la Fuente, J. M.; Feldmann, J.; Gaub, H. E.; Josephson, L.; Kagan, C. R.; Kotov, N. A.; Liz-Marzan, L. M.; Mattoussi, H.; Mulvaney, P.; Murray, C. B.; Rogach, A. L.; Weiss, P. S.; Willner, I.; Parak, W. J. The State of Nanoparticle-Based Nanoscience and Biotechnology: Progress, Promises, and Challenges. *ACS Nano* **2012**, *6*, 8468−8483.
(10) Gao, Z.; Lukyanov, A. N.; Singhal, A.; Torchilin, V. P. Diacyllipid-Polymer Micelles as Nanocarriers for Poorly Soluble Anticancer Drugs. *Nano Lett.* **2002**, *2*, 979−982.
(11) Stylianopoulos, T. EPR-effect: Utilizing Size-dependent Nanoparticle Delivery to Solid Tumors. *Ther. Delivery* **2013**, *4*, 421−433.
(12) Maeda, H.; Nakamura, H.; Fang, J. The EPR Effect for Macromolecular Drug Delivery to Solid Tumors: Improvement of Tumor Uptake, Lowering of Systemic Toxicity, and Distinct Tumor Imaging in vivo. *Adv. Drug Delivery Rev.* **2013**, *65*, 71−79.
(13) Liu, G.; Gao, J.; Ai, H.; Chen, X. Applications and Potential Toxicity of Magnetic Iron Oxide Nanoparticles. *Small* **2013**, *9*, 1533−1545.
(14) Jia, L.; Zhao, Y. L.; Liang, X. J. Fast Evolving Nanotechnology and Relevant Programs and Entities in China. *Nano Today* **2011**, *6*, 6−11.
(15) Huhn, D.; Kantner, K.; Geidel, C.; Brandholt, S.; De Cock, I.; Soenen, S. J.; Rivera Gil, P.; Montenegro, J. M.; Braeckmans, K.; Mullen, K.; Nienhaus, G. U.; Klapper, M.; Parak, W. J. Polymer-coated Nanoparticles Interacting with Proteins and Cells: Focusing on the Sign of the Net Charge. *ACS Nano* **2013**, *7*, 3253−3263.
(16) Kasai, H.; Murakami, T.; Ikuta, Y.; Koseki, Y.; Baba, K.; Oikawa, H.; Nakanishi, H.; Okada, M.; Shoji, M.; Ueda, M.; Imahori, H.; Hashida, M. Creation of Pure Nanodrugs and Their Anticancer Properties. *Angew. Chem., Int. Ed.* **2012**, *51*, 10315−10318.
(17) Zhang, J.; Li, Y.; An, F. F.; Zhang, X.; Chen, X.; Lee, C. S. Preparation and Size Control of Sub-100 nm Pure Nanodrugs. *Nano Lett.* **2015**, *15*, 313−318.
(18) Zhang, L. Y.; Yang, M.; Wang, Q.; Li, Y.; Guo, R.; Jiang, X. Q.; Yang, C. Z.; Liu, B. R. 10-Hydroxycamptothecin Loaded Nanoparticles: Preparation and Antitumor Activity in Mice. *J. Controlled Release* **2007**, *119*, 153−162.
(19) Niu, G.; Zhu, L.; Ho, D. N.; Zhang, F.; Gao, H.; Quan, Q.; Hida, N.; Ozawa, T.; Liu, G.; Chen, X. Longitudinal Bioluminescence Imaging of the Dynamics of Doxorubicin Induced Apoptosis. *Theranostics* **2013**, *3*, 190−200.
(20) Zhou, M.; Zhang, X.; Yang, Y.; Liu, Z.; Tian, B.; Jie, J.; Zhang, X. Carrier-free Functionalized Multidrug Nanorods for Synergistic Cancer Therapy. *Biomaterials* **2013**, *34*, 8960−8967.
(21) Zolotarskaya, O. Y.; Wagner, A. F.; Beckta, J. M.; Valerie, K.; Wynne, K. J.; Yang, H. Synthesis of Water-Soluble Camptothecin-Polyoxetane Conjugates via Click Chemistry. *Mol. Pharmaceutics* **2012**, *9*, 3403−3408.
(22) Liu, Z.; Robinson, J. T.; Sun, X. M.; Dai, H. J. PEGylated Nanographene Oxide for Delivery of Water-insoluble Cancer Drugs. *J. Am. Chem. Soc.* **2008**, *130*, 10876−10877.
(23) *Discovery Studio Modeling Environment, Release 4.0*. Accelrys Software Inc.: San Diego, 2013.
(24) Frederick, C. A.; Williams, L. D.; Ughetto, G.; van der Marel, G. A.; van Boom, J. H.; Rich, A.; Wang, A. H. Structural Comparison of Anticancer Drug-DNA Complexes: Adriamycin and Daunomycin. *Biochemistry* **1990**, *29*, 2538−2549.
(25) Lebwohl, D. E.; Canetta, R. New Developments in Chemotherapy of Advanced Breast Cancer. *Ann. Oncol.* **1999**, *10*, 139−146.
(26) Xue, X.; Zhao, Y.; Dai, L.; Zhang, X.; Hao, X.; Zhang, C.; Huo, S.; Liu, J.; Liu, C.; Kumar, A.; Chen, W. Q.; Zou, G.; Liang, X. J. Spatiotemporal Drug Release Visualized through a Drug Delivery System with Tunable Aggregation-induced Emission. *Adv. Mater.* **2014**, *26*, 712−717.
(27) Solntsev, K. M.; Sullivan, E. N.; Tolbert, L. M.; Ashkenazi, S.; Leiderman, P.; Huppert, D. Excited-state Proton Transfer Reactions of 10-hydroxycamptothecin. *J. Am. Chem. Soc.* **2004**, *126*, 12701−12708.
(28) Morgan, M. T.; Nakanishi, Y.; Kroll, D. J.; Griset, A. P.; Carnahan, M. A.; Wathier, M.; Oberlies, N. H.; Manikumar, G.; Wani, M. C.; Grinstaff, M. W. Dendrimer-encapsulated Camptothecins: Increased Solubility, Cellular Uptake, and Cellular Retention Affords Enhanced Anticancer Activity in vitro. *Cancer Res.* **2006**, *66*, 11913−11921.
(29) Kong, X.; Yu, K.; Yu, M.; Feng, Y.; Wang, J.; Li, M.; Chen, Z.; He, M.; Guo, R.; Tian, R.; Li, Y.; Wu, W.; Hong, Z. A Novel Multifunctional Poly(amidoamine) Dendrimeric Delivery System with Superior Encapsulation Capacity for Targeted Delivery of the Chemotherapy Drug 10-hydroxycamptothecin. *Int. J. Pharm.* **2014**, *465*, 378−387.
(30) Schmidt, M. Chemotherapy in Early Breast Cancer: When, How and Which One? *Breast Care* **2014**, *9*, 154−160.
(31) Sinclair, S.; Swain, S. M. Primary Systemic Chemotherapy for Inflammatory Breast Cancer. *Cancer* **2010**, *116*, 2821−2828.
(32) Endo, M.; Miwa, M.; Ura, M.; Tanimura, H.; Taniguchi, K.; Miyazaki, Y.; Ohwada, J.; Tsukazaki, M.; Niizuma, S.; Murata, T.; Ozawa, S.; Suda, H.; Ogawa, K.; Nanba, E.; Nagao, S.; Shimma, N.; Yamada-Okabe, H. A Water Soluble Prodrug of a Novel Camptothecin Analog is Efficacious Against Breast Cancer Resistance Protein-expressing Tumor Xenografts. *Cancer Chemother. Pharmacol.* **2010**, *65*, 363−371.
(33) Nogi, H.; Kobayashi, T.; Tabei, I.; Kawase, K.; Toriumi, Y.; Suzuki, M.; Morikawa, T.; Uchida, K. The Predictive Value of PgR and HER-2 for Response to Primary Systemic Chemotherapy in Inflammatory Breast Cancer. *Int. J. Clin. Oncol.* **2008**, *13*, 340−344.
(34) Riganti, C.; Voena, C.; Kopecka, J.; Corsetto, P. A.; Montorfano, G.; Enrico, E.; Costamagna, C.; Rizzo, A. M.; Ghigo, D.; Bosia, A. Liposome-Encapsulated Doxorubicin Reverses Drug Resistance by Inhibiting P-Glycoprotein in Human Cancer Cells. *Mol. Pharmaceutics* **2011**, *8*, 683−700.
(35) Komarova, N. L.; Wodarz, D. Drug Resistance in Cancer: Principles of Emergence and Prevention. *Proc. Natl. Acad. Sci. U. S. A.* **2005**, *102*, 9714−9719.

DOI: 10.1021/acsami.5b05347
ACS Appl. Mater. Interfaces 2015, 7, 19295−19305

(36) Xu, X.; Li, R. B.; Ma, M.; Wang, X.; Wang, Y. H.; Zou, H. F. Multidrug Resistance Protein P-glycoprotein Does Not Recognize Nanoparticle C-60: Experiment and Modeling. *Soft Matter* **2012**, *8*, 2915−2923.
(37) Yusa, K.; Tsuruo, T. Reversal Mechanism Of Multidrug Resistance by Verapamil - Direct Binding Of Verapamil To P-Glycoprotein on Specific Sites And Transport Of Verapamil Outward across the Plasma-Membrane Of K562 Adm Cells. *Cancer Res.* **1989**, *49*, 5002−5006.
(38) Park, H. W.; Park, H.; Semple, I. A.; Jang, I.; Ro, S. H.; Kim, M.; Cazares, V. A.; Stuenkel, E. L.; Kim, J. J.; Kim, J. S.; Lee, J. H. Pharmacological Correction of Obesity-induced Autophagy Arrest Using Calcium Channel Blockers. *Nat. Commun.* **2014**, *5*, 4834−4858.
(39) Kaufmann, S. H. Antagonism between Camptothecin and Topoisomerase II-directed Chemotherapeutic Agents in a Human Leukemia Cell Line. *Cancer Res.* **1991**, *51*, 1129−1136.
(40) Gracz, A. D.; Johnston, M. J.; Wang, F. C.; Williamson, I. A.; Wang, Y. L.; Balowski, J.; Sims, C.; Li, L. H.; Allbritton, N.; Magness, S. T. An in vitro Assay for Clonogenic, High-throughput Analysis of Intestinal Stem Cells. *FASEB. J.* **2012**, *26*, 340−349.
(41) Tan, K. B.; Mattern, M. R.; Eng, W. K.; Mccabe, F. L.; Johnson, R. K. Nonproductive Rearrangement of DNA Topoisomerase-I and Topoisomerase-Ii Genes - Correlation with Resistance to Topoisomerase Inhibitors. *J. Natl. Cancer Inst.* **1989**, *81*, 1732−1735.
(42) Sugimoto, Y.; Tsukahara, S.; Ohhara, T.; Liu, L. F.; Tsuruo, T. Elevated Expression of DNA Topoisomerase-Ii in Camptothecin-Resistant Human Tumor-Cell Lines. *Cancer Res.* **1990**, *50*, 7962−7965.

DOI: 10.1021/acsami.5b05347
ACS Appl. Mater. Interfaces 2015, 7, 19295−19305